AWESW2022
21st Australasian Wind Engineering Society Workshop
2 – 3 February, 2023

Adelaide Oval Lighting Upgrade – Wind Assessment

Neil Mackenzie[1], Parivash Shams-Abadi[2] Sam Daniels[3], Gabriel McGrane[4], Eugene Cullity[5], James Rhodes[6], Benjamin Bleckley[7]

[1]neil.mackenzie@mottmac.com; [2]Parivash.shams-abadi@mottmac.com;
[3]sam.daniels@mottmac.com;.[4]gabriel.mcgrane@mottmac.com; [5]eugene.cullity@mottmac.com;
[6]james.rhodes@mottmac.com; [7]Benjamin.bleckley@mottmac.com

ABSTRACT

Adelaide Oval is investigating the feasibility of upgrading the existing HID (High Intensity Discharge) lights mounted to each headframe on each tower, to LED lights which are fewer in number but larger in size, more energy efficient, reduced operational cost while improving resilience, and enhanced game day experience. Despite requiring a lesser number of fittings with an LED arrangement, the total resultant sail area of the light tower head frames will increase by approximately double as the fixtures themselves are larger as is the overall size of the headframe. This paper outlines the assessment of wind loads regarding serviceability deflections, ultimate strength, and fatigue. This work involved site surveys, wind tunnel measurements, dynamic analysis, and code comparisons.

1. Introduction

Adelaide Oval is a sensitive sporting venue, with the local community in North Adelaide preventing various attempts to upgrade the stadium due to potential noise and light emissions, and Adelaide City Council preventing upgrades as the parklands surrounding the city were part of Colonel William Light's vision to create a green belt around the city. Given community concerns, light towers were eventually given consent in 1997, with retractable towers used to defuse community and council concerns. Unfortunately, these towers were plagued with technical difficulties, at one time accidentally collapsing and others the jacking mechanism jamming.

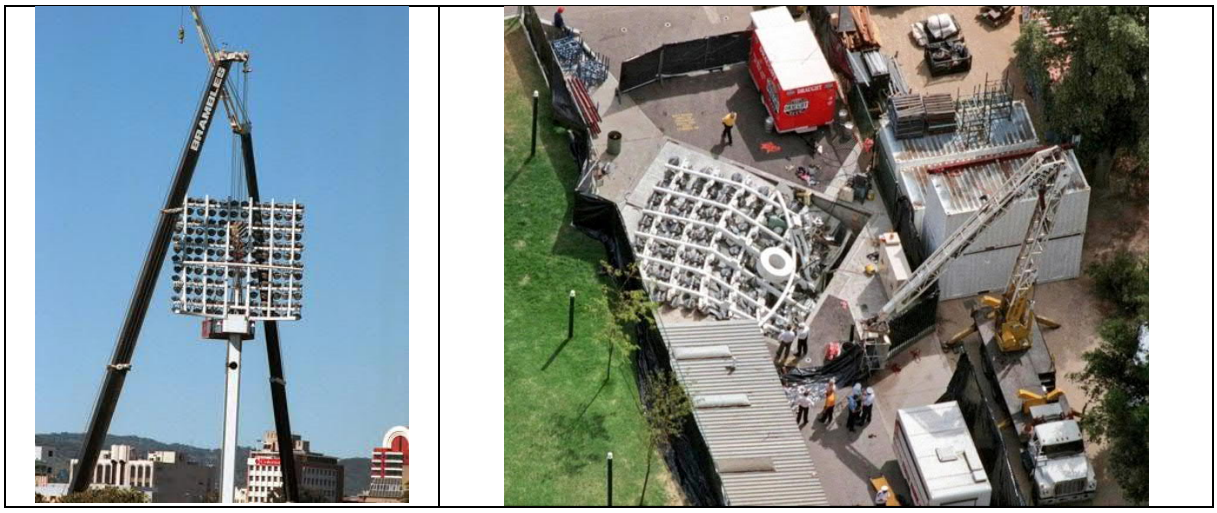

Figure 1 Original Adelaide Oval Light Towers

They were replaced with permanent/fixed towers of steel hollow section, tapered in diameter with height, prior to the redevelopment in 2010, and subsequently integrated into the new development as shown below

Following on from the success of the 2017 Technology Upgrade at Adelaide Oval, which included the upgrade of the sports lighting fixtures mounted on the leading edge of the West, South and Eastern Stands to LED (Light Emitting Diode), Adelaide Oval is investigating the feasibility of upgrading the remaining HID (High Intensity Discharge) tower-based sports lighting to LED. The benefits of the upgrade include improved energy efficiency (by about 50%), reduced operational cost

Figure 2 New light towers at Adelaide Oval integrated into the redevelopment

2. Previous Work

Kwok et al (1985) carried out dynamic testing of light towers at the Sydney Cricket Ground, New South Wales, with the first two modes (longitudinal and lateral sway) at measured at 0.5Hz, second two at ~2.4Hz and next two at ~4.8Hz. These compared favorably with those estimated using a finite element model. The towers were similar in form to those at Adelaide Oval, being a steel tapered tubular structure, with an external diameter of 3m (10mm thick) at the base tapering to 1.5m (5mm thick) at the top (65m height). The headframe was 10m high and 5m wide, with 70 lights mounted on the headframe. Critical damping ratio of ~0.25-0.35% was measured for the first two modes, increasing to ~1% for subsequent modes.

Mackenzie et al (2012) derived equivalent static wind loads in the along and cross wind directions for proposed upgrade of AAMI stadium (now demolished following the redevelopment of Adelaide Oval) at West Lakes in South Australia. The tower is of similar height to that at the SCG at 60m, with the diameter varying from 2.5m at the base to 1.34 at the top, and steel thickness varying from 12mm at the base to 6mm thick at the top. The proposed upgrade involved augmenting (lifting and extending at the base with a new 20mm thick section of similar diameter), extending at the top, and stiffening the tower to extend the life of existing towers, with all options including a new headframe and lights.

- The first two modes varied from ~0.34Hz for augmented, 0.29Hz for stiffened and 0.24Hz for existing. These were estimated using a finite element model and not measured.
- Along wind loads were derived using Holmes and Kesperski (1996) and Holmes (1996b).
- Aerodynamic damping was derived using Holmes (1996a) and found to contribute an additional 3% relative to structural damping of 1% (as per AS1170 (2021)).
- Both synoptic and downdraft wind speeds and profiles were considered, with thunderstorm downdraft winds dominant for return periods greater than about 10 years. Base loads were about 10% greater for synoptic the downdraft winds.

- Drag coefficients were measured using a 1:50 scale model of the headframe and found to be less than that estimated using the wind code, AS 1170.2 (2021). The solidity ratio was estimated at 50% giving a code estimate of drag ~20% greater than that measured. Letchford (2001) proposed a different exponent for the cladding reduction factor, with the exponent, α, in equation (1) below equal to 2.0 in AS1170.2(2021) compared with Letchford's proposal of 1.5.

$$K_p = 1 - (1 - \delta)^{\alpha} \quad (1)$$

  EN 1991-1-4 (2010) notes "For solid walls the solidity φ should be taken as 1, and for walls which are 80 % solid (i.e. have 20 % openings) φ = 0,8. Porous walls and fences with a solidity ratio φ ≤ 0,8 should be treated as plane lattices"
- The cross-wind response due to vortex shedding was calculated using AS1170.2 (2021) and Bolton's (1994) formula which indicated deflections of ~100mm (0.5% damping).

The same approach was used in Gaekwad and Mackenzie (2013), "Dynamic Assessment of Wind Sensitive Stadium Structures", for new light towers at Simonds Stadium (now GMHBA) in Geelong, Victoria. Subsequent to this work, Mackenzie et al (2016) also used EN 1991-1-4 (2010) to assess cross-wind effects due to vortex shedding, including deflection and number of cycles over the life-span of the structure.

3. Headframe Drag Coefficients

3.1 Headframe Alternatives and Code Estimates

Three lighting configurations on the headframe have been proposed, "Existing" with HID lights, "LED#1" as an alternative with LED lights, and "LED#2" as a competing alternative with LED lights. These are shown below in Figure 3, as 3D digital (Rhino) models. Solidity ratios were determined accurately using an algorithm to count pixel colour as shown below in Figure 4, with AS1170.2 (2021) then used to derive drag coefficients (assuming the headframe can be considered as a porous hoarding) as shown below in Table 2. An alternative approach would be to assess drag on each light fitting, which would lead to a much greater overall drag coefficient.

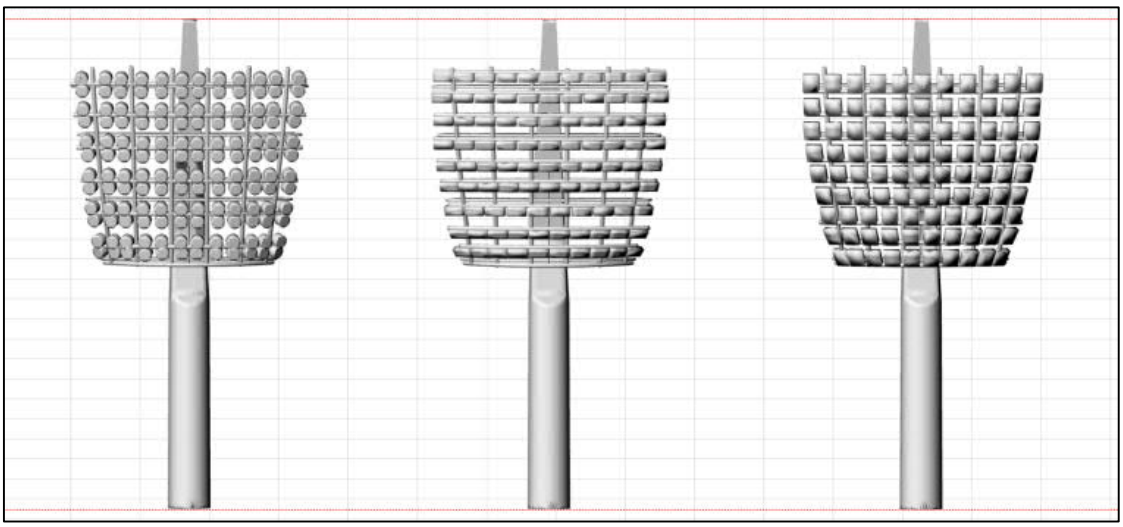

Figure 3 3D models of each headframe (Existing, LEFT, LED#1, centre, LED#2, right)

Table 1 Headframe properties

Lighting Option	Fixture Qty	Fixture Mass (kg)	Headframe Mass (kg)	Total Mass (kg)
Existing	144	12	3,215	8,110
LED 1	96	24	3,440	5,740
LED 2	94	26.5	3,440	6,540

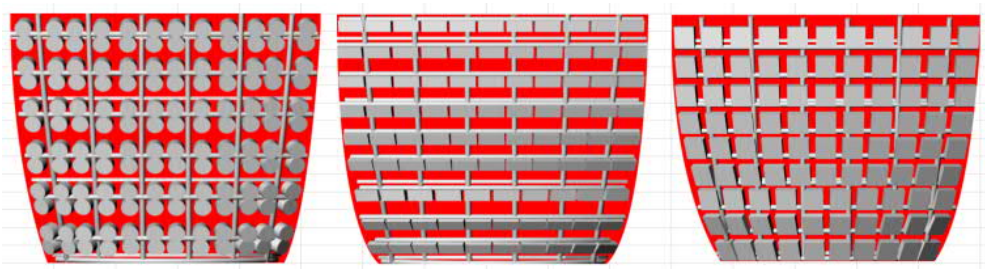

Figure 4 Pixelated image used to derive solidity ratio.

3.2 Wind Tunnel Test

A 1:50 scale model of the proposed headframes were 3D printed and placed in the University of Sydney's boundary layer wind tunnel for base load analysis. The model was placed on a JR3 Force-Moment Sensor and was orientated in the tunnel. The turntable was then turned clockwise and measurements of the base forces and moments were made every 10° using a data acquisition system that sampled at 400Hz (with the signals filtered at 200Hz). The resultant of the X and Y components of the force recorded in the wind tunnel was used to determine the drag coefficient on the structure for the headframe and supporting pole attached. Drag on the pole was measured separately and deducted. The results are shown below in Figure 6, along with code estimates of drag coefficient (for wind incident perpendicular to the headframe). It's interesting to note that there is little reduction with wind from the read of the headframe for LED#2, however there is a sifnificant reduction for the existing and LED#2 headframes.

Drag coefficients estimated based on AS1170.2 (exponent of 2.0 in equation (1)), EN1991-1-4 (with porosity reduction factor of 0.8) and measured are provided in Table 2. AS1170.2 overestimates drag by ~30%, with EN1991-1-4 less conservative at ~5-15%. Also worth noting is the slight increase in drag with height of about 5% (based on AS1170.2).

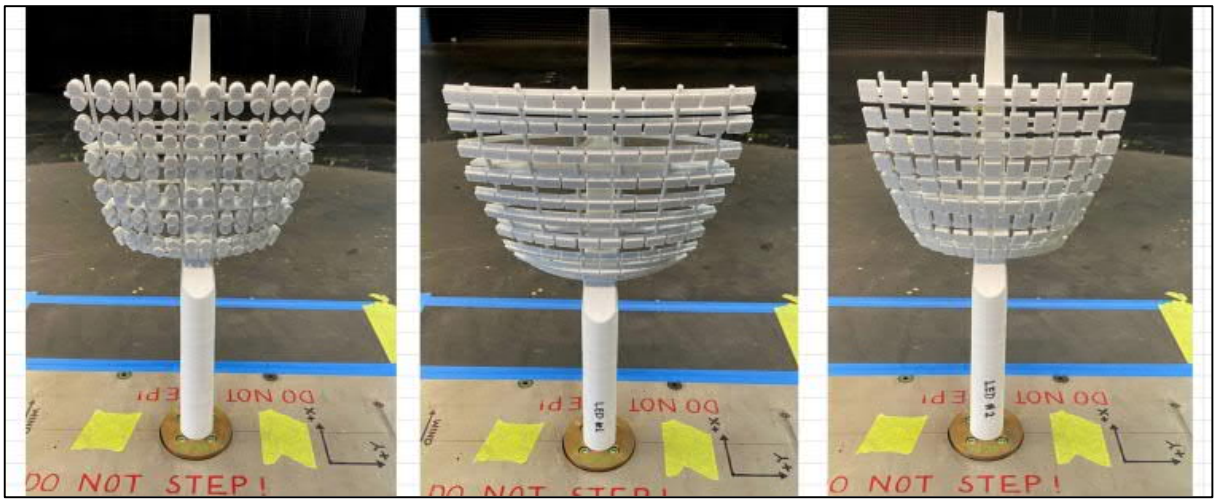

Figure 5 3D printed models of each headframe (Existing, LEFT, LED#1, centre, LED#2, right)

Table 2 Comparison of drag coefficients measured and estimated based on code

Headframe	Area (sqm)	Solidity Ratio	K_p (as per AS1170.2)	Calculated Drag Coefficient (Model)		Measured Drag Coefficient (Model)	Calculated Drag Coefficient (Full Scale)
				AS1170.2	EN1991-1-4		
Existing	56.4	84%	0.97	1.32	1.09	1.0	1.39
LED#1	57.3	72%	0.92	1.25		0.94	1.32
LED#2	57.0	77%	0.95	1.28		1.02	1.35

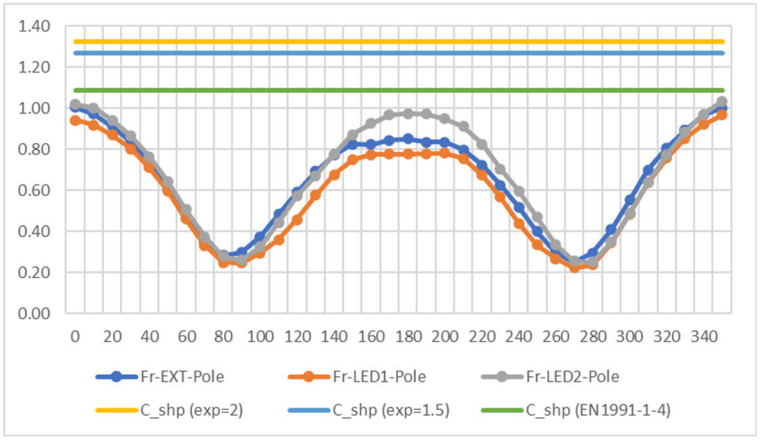

Figure 6 Measured drag coefficients compared with predicted (for existing)

4. Site Survey

A site survey was carried out to measure the steel thickness up the height of the tower using an ultrasonic thickness sensor, as well as the response of the tower using accelerometers aligned with each axes and an anemometer. The results of the tower response and accelerometer locations on the headframe are shown below in Figure 7, with a dominant frequency of ~0.50Hz evident, background response at ~0.1Hz and an additional response at ~2.6Hz (corresponding to the 7th mode and likely excited by vortex shedding, with the mean wind speed at the top of the tower ~10m/s). Steel thickness was measured as reducing from 26mm at the base to 13mm at the top)

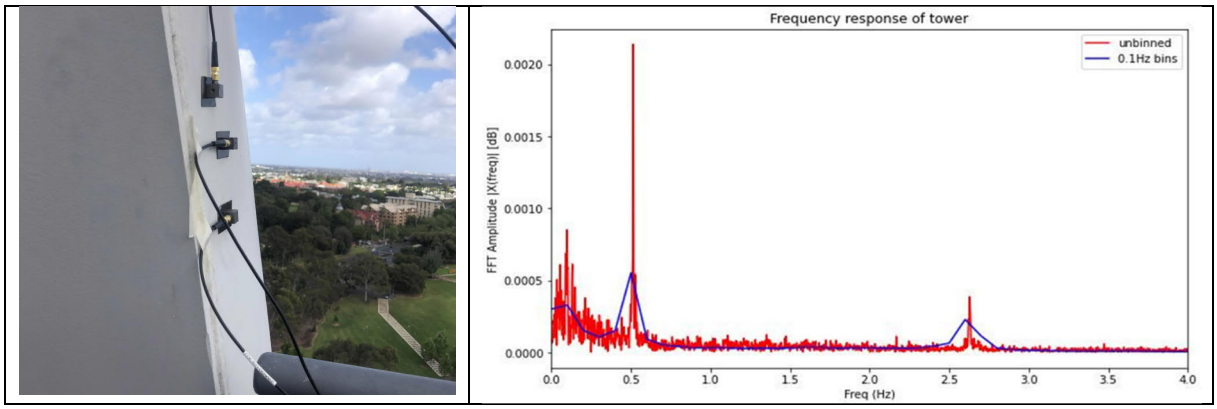

Figure 7 Site measurements

5. Dynamic Analysis

A finite element model of the tower was constructed in ETABS, a finite element modelling software (https://www.csiamerica.com/products/etabs), using the dimensional and physical properties for the tower, headframe and lights (shown below in Figure 8), with predicted modal frequencies shown below in Table 3. Mode shapes are visualized in Figure 9, with the first two modes sway. A mode shape of the form $\varphi(z) = (z/h)^{\beta}$ was fitted to the normalized displacement, with $\beta \approx 2.0$. Estimated modal frequencies compared well with those measured and those calculated by theory.

Table 3 Predicted modal frequencies

Mode	Existing	LED 1	LED 2
1	0.499	0.534	0.529
2	0.507	0.540	0.534
3	1.406	1.634	1.626

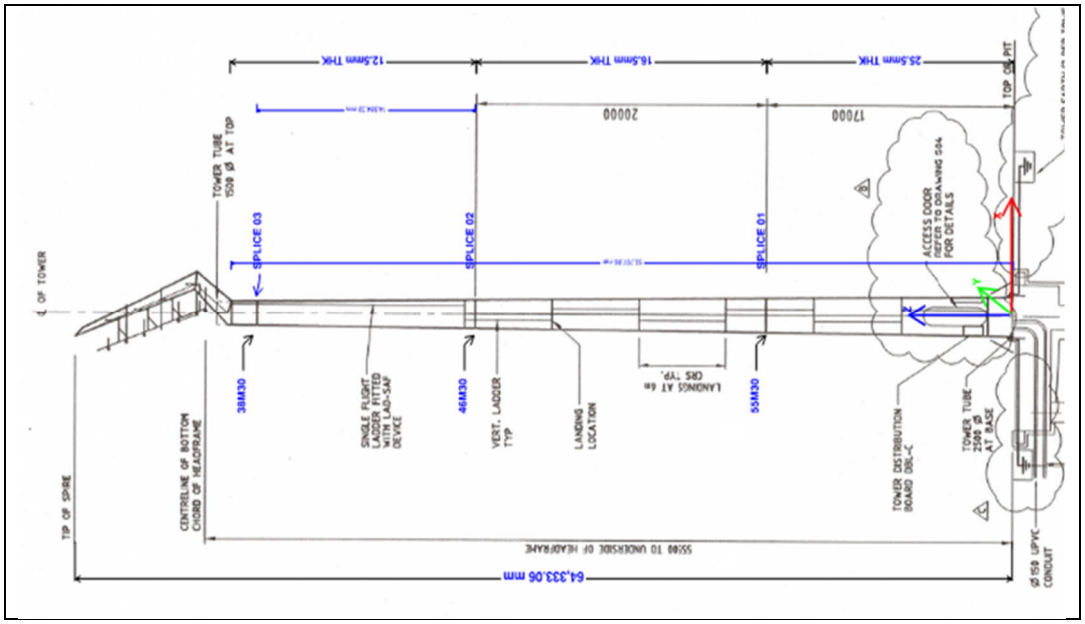

Figure 8 Tower dimensions

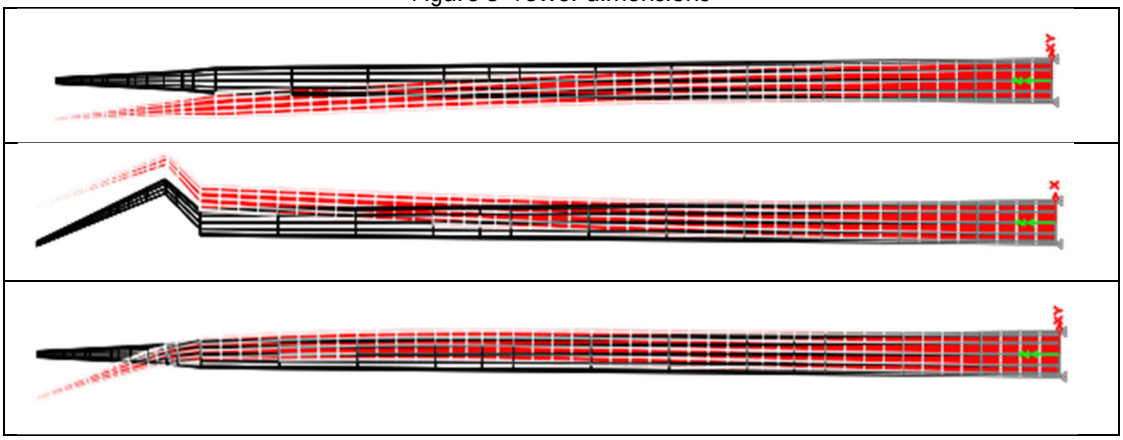

Figure 9 Mode shape visualisation

6. Derived Wind Loads

Reference is made to Gaekwad and Mackenzie (2013) and equations referenced therein:

- The mean load was calculated discretely using equation (27), with the mean velocity distribution defined using equation (2);
- The background load was calculated using equation (26), with the correlation coefficient able to be derived efficiently given the headframe dominated the response. Hence correlation of loads not associated with the headframe could be ignored. The resulting correlation coefficient was derived as using equation (29);
- The resonant load was calculated using equation (25).

Results of the analysis are shown below in Table 4, as components (mean, background and resonant) and in total.

Table 4 Reactions (Moments) at the tower base

Headframe	Mean (kNm)	Background (kNm)	Resonant (kNm)	Total (kNm)
Existing	3137	3292	1770	6959
LED#1	3009	3142	1593	6653
LED#2	3180	3343	1683	7039

7. Structural Analysis

The equivalent static wind loads derived above were applied discretely to the ETABS model, with the resulting stresses for serviceability (25 year return period wind speed) and ultimate (500 year return period wind speed) given below in Figure 10 (circumferential and longitudinal). Ultimate stress of ~72MPa is less than the limit of 250MPa.

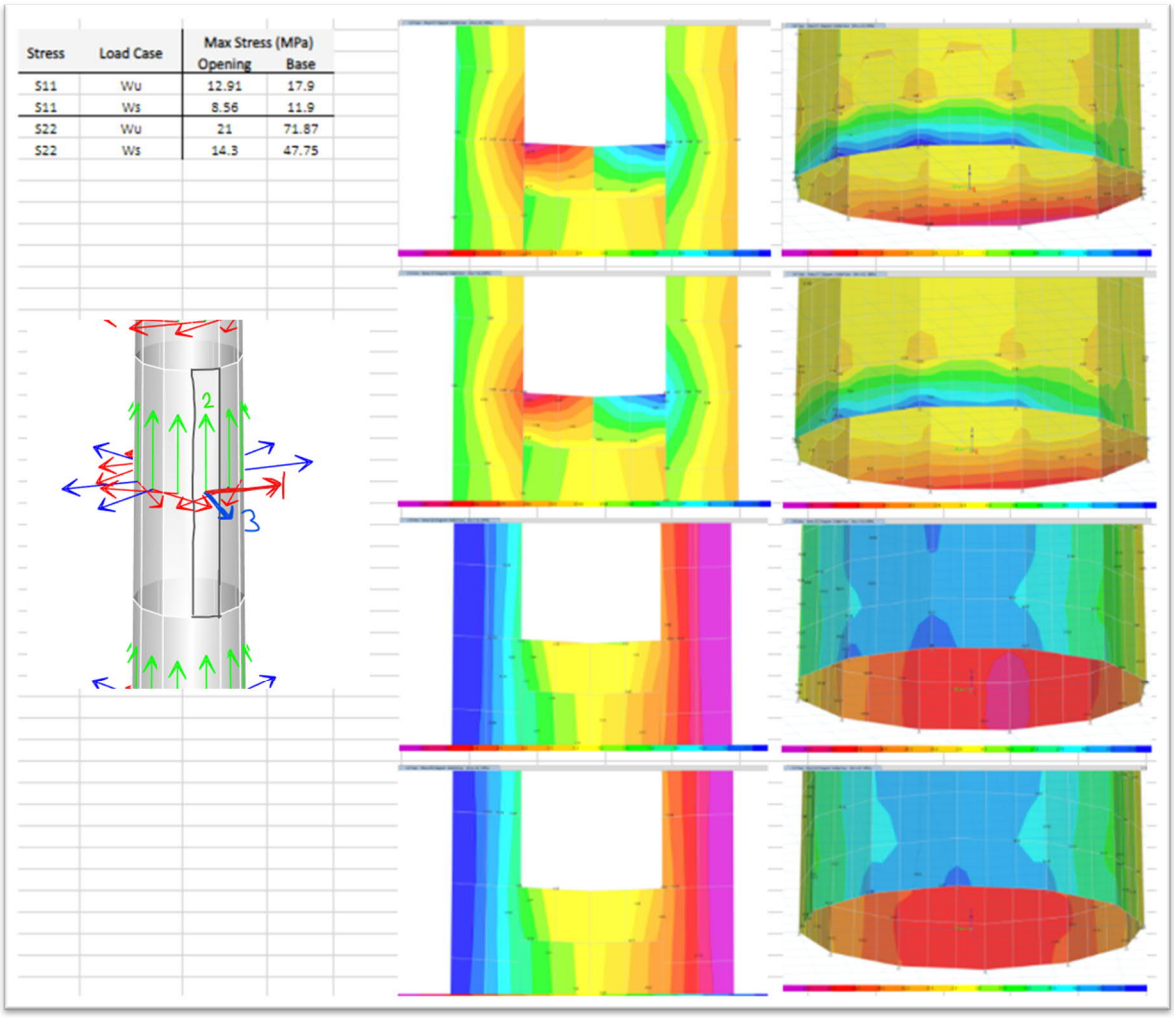

Figure 10 Stress Analysis (Ultimate, wu, and serviceability, ws)

Additionally, deflections due to the serviceability loads were also estimated as per Table 5, with ~500mm deflection corresponding to ~50MPa. The deflection marginally complies with serviceability limits prescribed in AS4100 (2020) of h/150 or ~500mm (based on height of tower being 75m).

Table 5 Deflections with serviceability wind speed

Loading	Deflection (mm)		
	Existing	LED 1	LED 2
Serviceability	448	424	454
Serviceability + Gravity	490	450	479

8. Fatigue Analysis

Previously Holmes (1998) reviewed two classes of methods for the calculation of the cross-wind response of structures due to vortex shedding. These approaches have been formalised in EN 1991 (2010) and are outlined below. A comparison of the application of these methods in different international codes is given in Muñoz Black et al (2009). Both methods rely on the definition of the generalised force on the structure as the integral of the product of the inertia force in the cross-wind direction with the mode shape across the height, h of the structure as detailed in Gaekwad and Mackenzie (2013).

In this case the inertial force is assumed to be of sinusoidal form, with Ruscheweyh (1988) including the effects of correlation length (this concept is also outlined in Gaekwad and Mackenzie (2013)) to give the ratio of maximum displacement to cylinder diameter (y_{max}/D) as:

$$\frac{y_{max}}{D} = \frac{1}{St^2}\frac{1}{Sc} K K_w C_{lat} \tag{2}$$

With K the mode shape factor, K_w the correlation length factor, and C_{lat} the lateral force coefficient. The mode shape factor and correlation length factor can be derived from the mode shape, with the Strouhal, St, and Scruton, Sc, numbers derived as per EN 1991-1-4 or similar.

To assess fatigue, EN 1991 also provides an estimate for the number of load cycles, N, caused by vortex excited oscillations which can be compared with:

$$N = 2T f_c \varepsilon_0 \left(\frac{V_{crit}}{c}\right)^2 exp\left(-\left(\frac{V_{crit}}{V_0}\right)^2\right) \tag{3}$$

With ε_0 the bandwidth factor describing the band of wind velocities with vortex-induced vibrations, T the lifetime of the structure (in seconds), V_{crit} the critical wind speed (m/s) for "lock-in" (coincidence of vortex shedding frequency with natural frequency) and V_0 times the modal value of the Weibull probability distribution assumed for the wind velocity (m/s).

Using EN1991-1-4, the maximum deflection (with a critical damping ratio of 1%) due to vortex shedding was determined to be less than 50mm, corresponding to a stress of ~5MPa (pro-rata with serviceability deflection/stress). The number of stress cycles was estimated to be ~5e8 based on a lifetime of 70 years (50 year life extension from present with upgraded headframe). This is within the limits prescribed by AS4100 for fatigue stress with non-redundant load paths (factored by 0.7) and load cycles.

9. Conclusions

Adelaide Oval is investigating the feasibility of upgrading the existing HID (High Intensity Discharge) lights mounted to each headframe on each tower, to LED lights which are fewer in number but larger in size, more energy efficient, reduced operational cost while improving resilience, and enhanced game day experience. Despite requiring a lesser number of fittings with an LED arrangement, the total resultant sail area of the light tower head frames will increase by approximately double as the fixtures themselves are larger as is the overall size of the headframe. Drag coefficients were measured and found to be ~30% less than code estimates (AS1170.2), with EN1991-1-4 found to provide more accurate estimates of drag based on porosity. Wind loads were derived using the method outlined by Holmes (2015) and when applied to the structure serviceability deflections were found to be the governing design criterion, with ultimate stress well within limits and fatigue not required to be assessed.

10. Acknowledgements

We would like to acknowledge our client, Stadium Management Authority, for giving us the opportunity to work on this project and site access, and Mott MacDonald's Project Director and Built Environment leader for South Australia. We also acknowledge the University of Sydney's assistance with access to their wind tunnel and instrumentation. Finally, others that participated as part of our Engineering Sciences team, including Moharis Kamis etc.

References

EN 1991-1-4:2005+A1:2010 (2010) "Eurocode 1: Actions on structures - Part 1-4: General actions – Wind actions", CEN

Gaekwad, J. and Mackenzie, N.C. (2013) "Dynamic Assessment of Wind Sensitive Stadium Structures", Proceedings of Australian Acoustics Conference, Victor Harbor, SA, Australia.

Holmes J D (1996a). "Along-wind response of lattice towers - II. Aerodynamic damping and deflections." Engineering Structures, Vol. 18, No. 7, pp. 483-488.

Holmes J D (1996b). "Along-wind response of lattice towers, III: Effective load distributions". Engineering Structures, Vol. 18, pp 489-494.

Holmes J D, Kasperski M, (1996), "Effective distributions of fluctuating and dynamic wind loads". Australian Civil/Structural Engineering Transactions. Vol. CE38, pp 83-88.

Holmes, J.D., (1994), "Along-wind response of lattice towers: Part I – Derivation of expressions for gust response factors", Engineering Structures, Vol 16, No 4, pp 287-292.

Kwok, K.C.S., Hancock, G.J., Bailey, P.A. and Haylen, P.T., (1985), "Dynamics of a freestanding steel light tower", Eng. Struct., Vol. 7 (Jan), pp 46-50.

Letchford, C. W., (2001), "Wind Loads on Rectangular signboards and hoardings", Journal of Wind Engineering and Industrial Aerodynamics, Vol. 89 No. 2, pp 135-151

Mackenzie, N.C. and Tanner, K.E., (2016), "Crosswind response of cylindrical towers with strakes", Australasian Wind Engineering Society Workshop, 6-8 July 2016.

Muñoz Black, C.J., Barrios, H.H. and López, A.L. (2009) "A comparison of cross-wind response evaluation for chimneys following different international codes", 11th Americas Conference on Wind Engineering, San Juan, Puerto Rico

Ruscheweyh H. and Sedlacek G. (1988) "Crosswind vibrations of steel stacks-critical comparison between some recently proposed codes", Journal of Wind Engineering and Industrial Aerodynamics, Vol.30, p. 173-183

Standards Australia, (2020), "Structural design actions. Part 2 Wind actions", Australian/New Zealand Standard, AS/NZS 4100:2020.

Standards Australia, (2021), "Structural design actions. Part 2 Wind actions", Australian/New Zealand Standard, AS/NZS 1170.2:2021.